Thermochimica Acta, 84 (1985) 123–131
Elsevier Science Publishers B.V., Amsterdam – Printed in The Netherlands

FURTHER INVESTIGATION ON THE PHOTOELECTRIC AND DIELECTRIC PROPERTIES OF HgTe–CdTe SOLID-SOLUTION THIN FILM FOR SOLAR CELLS

A. TAWFIK, M.I. ABD EL-ATI and M.M. ABOU SEKKINA *

Physics and Chemistry Departments, Faculty of Science, Tanta University, Tanta (Egypt)

(Received 16 August 1984)

ABSTRACT

A homogeneous thin film of composition $Hg_{(1-x)}Cd_xTe$ was prepared by vacuum evaporation on a glass substrate using an indium contact. On this material, several measurements were made, comprising the temperature dependence of AC-electrical conductivity, the temperature and frequency dependences of the dielectric constant, photo-conductivity and current–voltage characteristics.

The results obtained were promising and indicative of a good conformity between the value of ΔE as newly determined from current–voltage relationships and that previously determined from the temperature dependence of conductivity data.

The mobility of charge carriers was determined to be 1.97×10^{-7} cm^2 V^{-1} s^{-1} associated with a donor concentration of 4.5×10^{18} cm^{-3} and a high-temperature activation energy of 0.078 eV. These values are indicative of a localized state conduction (hopping) mechanism.

The material prepared shows a good response for light exposure which enables it to be used for light detectors or the production of photosensors in photoelectric devices.

INTRODUCTION

The interest of the present study is promoted by the wide and useful application of HgTe films in photoelectric devices.

In accordance with the previous discussions of Mott [1] and Cohen [2], the application of Anderson's theory [3] for the effect of disorder on the nature of eigenstates in covalently bonded materials should give rise to a band-tail region of localized states and a region in which the states are extended. In the band tail the carriers are localized and move by phonon-assisted hopping which is in the energy range above the mobility edge. Carriers are in extended states and can diffuse throughout the material without phonon assistance, but with short mean-free-paths.

* Author to whom for correspondence should be addressed.

0040-6031/85/$03.30

CdTe and HgTe are zinc blende type crystals of the isoelectronic sequence II–VI and thus form mixed crystals in all proportions of the constituents Cd, Te and Hg. Alloys of general composition ($Hg_{(1-x)}Cd_xTe$) have a forbidden electron band ΔE dependent on x. However, an interesting feature of these alloys is that ΔE can be adjusted at an arbitrary low value for a suitable choice of the composition [4].

Narrow-gap semiconductors have helped this compound to be used in photodetection applications [5], which has led to the consideration of mixed systems with mercury-rich alloys.

The temperature dependence of the DC conductivity of $Hg_{(1-x)}Cd_xTe$ was previously studied [6]. The activation energy was about 0.09 eV for the thin film.

To determine the relative importance of conduction in localized and extended states, it is obviously necessary to make extensive measurements of many properties on well-characterized samples of a given amorphous material. In this paper we report the results of such a study of the transport properties of amorphous mercury cadmium telluride, comprising current–voltage characteristics, temperature dependence of the electrical conductivity, temperature dependence of the dielectric constant and photoconductivity as a function of applied field and distance (energy) from the UV light source (265 nm).

In the present investigation the AC conductivity and dielectric constant against temperature are studied. Another reason for studying the effect of universal temperature on the logarithm of the DC current passing through the thin film, is to calculate the mobility of the carriers and density of the donors, besides the thickness of the depletion layer. All of these are good semiconducting parameters.

EXPERIMENTAL TECHNIQUES

Material preparation

$Hg_{(1-x)}Cd_xTe$ thin-film structures were deposited on a glass substrate held at a temperature of $\simeq 100°C$ in vacuum ($1–5 \times 10^{-6}$ Torr) using a Balzers BA 510 coating unit. Molybdenum boats were used for evaporating the materials and indium electrodes were used for deposition.

The dimensions of the thin films are 0.3 cm^2 area and 0.1 μm thickness.

Electrical measurements

The DC-bias voltage was provided by a DC-power supply (Levell) and current was recorded by an electronic Avometer (No. 2658772).

The voltage drop across the sample was recorded with a DC microvoltmeter (type TM10). Sample temperature was monitored with a contact thermometer attached to the substrate.

Dielectric measurements

The dielectric constant was determined using a signal generator (type TRI_0AG-203) and an electronic Avometer (No. 2658772) to record the AC voltage at different frequencies.

The AC current was recorded by an Avometer (No. 2658772) and as a function of temperature.

The dielectric constant was determined from the following

$$\frac{I}{\omega V} = \frac{\epsilon A}{4\pi d} \qquad \epsilon = \frac{4\pi dI}{\omega VA}$$

where V = the AC voltage drop on the sample; A = the area of the sample surface; d = the thickness of the film; I = the current; ω = the measured frequency = $2\pi f$.

RESULTS AND DISCUSSION

Figures 1 and 2 show the variation of the dielectric constant (ϵ) with temperature at different frequencies. It is clear that an increase in temperature causes an increase in the dielectric constant values obtained. This could be correlated with the induced and increased thermal polarization of the thin films in the same direction (Fig. 1). Conversely to this behaviour, an increase in the frequency may cause a decrease in the dielectric constant values

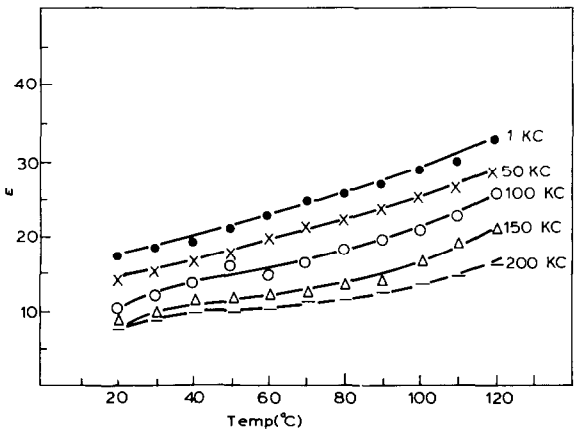

Fig. 1. Variation of the dielectric constant as a function of temperature at various frequencies.

obtained for all curves as a general trend (Fig. 2). This is most probably correlated with the DC conduction, since the increase in frequency of the AC applied field may accelerate and activate the micro-Brownian motion [7] of the electric dipoles. This in turn increases the relaxation time of the electric dipoles and thus the charge may have a sufficient time to traverse the distance between the electrode surfaces to neutralize them. Thus, the net result is a drop in dielectric constant values.

Figure 3 illustrates the variation of logarithmic AC-electrical conductivity as a function of temperature at various frequencies. It is clear that all curves

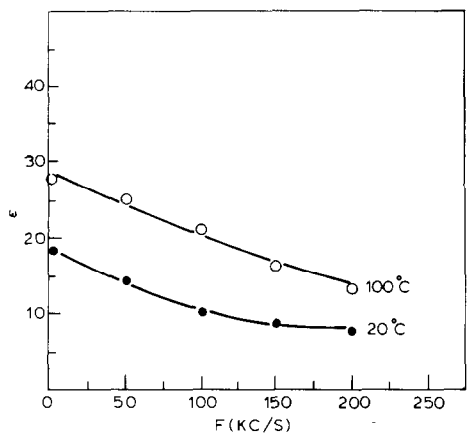

Fig. 2. Variation of dielectric constant as a function of frequency at 20 and 100°C.

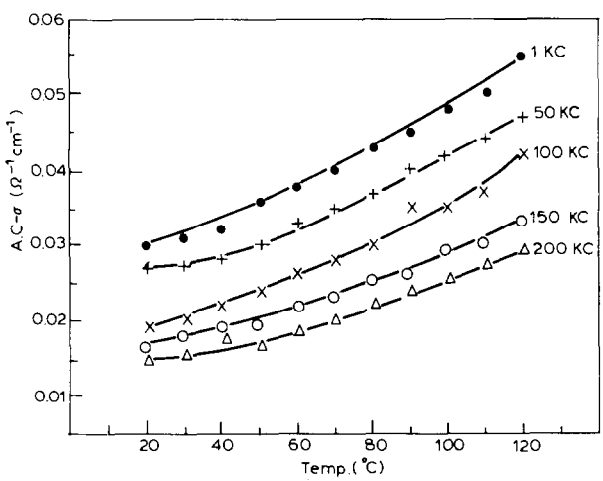

Fig. 3. Variation of AC electrical conductivity as a function of temperature at various frequencies.

have a general trend, namely an increase in electrical conductivity takes place with temperature. This proves that the material possesses a semiconducting conduction mechanism.

It is clear that the electrical conductivity decreased and the activation energy for conduction alters with increasing frequency. This could probably be correlated with the interaction of the grain boundary with the AC field.

Figure 4 indicates the variation of photoelectric current as a function of time of exposure to the mercury lamp ($\lambda = 265$ nm) at various applied DC voltages.

Figure 5 represents the distance dependence of photoelectric current at various applied DC voltages for HgTe–CdTe solid-solution films at various light intensities.

In summary, all curves of Fig. 4 have the following common trends.

(a) The curves are characterized by an initial rise in the photoelectric current with increasing exposure time till reaching constancy (saturation stage) at ~ 20 min exposure. This could be ascribed to the increased mobilization of Hg vacancies. Further light exposure may increase the potential barrier which inhibits the formation of Hall vacancies thus leading to a saturation state (~ 20 min).

(b) The increase in applied DC voltage causes an increase in the photocurrent which is correlated with the acceleration of Hg-vacancy mobilization and/or creation of further Hg vacancies.

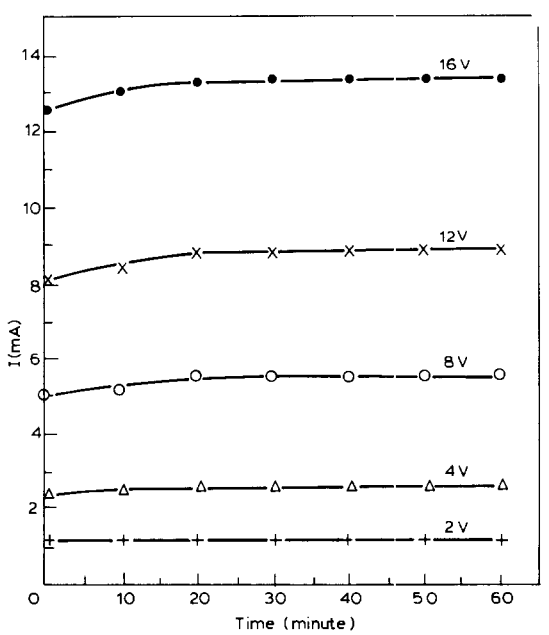

Fig. 4. Variation of the generated photoelectric current as a function of time of light (UV) exposure at various applied voltages.

(c) The saturation of the photo-current is observed at sufficiently high bias voltage, depending on the level of the light intensity.

(d) The remarkable characteristic of the photo-current is that a threshold voltage exists for the appearance of the photo-current. This is thought to be partly due to the electric field distribution in the region where the incident light is strongly absorbed and partly due to the length of the "schubweg" of the photoexcited holes.

Figure 5 indicates the variation of photo-current (I/mA) with distance (cm) from the Hg lamp. The behaviour of all curves of this figure indicates that the photo-current is initially decreased with increasing distance from the light source followed by near constancy at around a distance of 20 cm. This could be ascribed to the fact that the photoelectric energy decreases with increasing distance, till reaching a saturation state beyond which the photoelectric energy is not powerful enough to affect Hg-vacancy migration and/or Hg-vacancy creation.

On shortening the distance and increasing the exposure time, the illumination light intensity is substantially increased. At relatively high illumination intensity (Figs. 4 and 5), when temperature-independent bimolecular recombination takes place [8], the exponential temperature dependence of the photoconductivity must arise from one of two causes: (1) possibly a fraction of the carriers proportional to $\exp[-(E_c - E_A)/KT]$ may be activated above the mobility edge, and only they contribute to the current [9]; (2) alternatively, the carriers may have an activated mobility in the bimolecular regime. It is now suggested that the latter explanation is more likely.

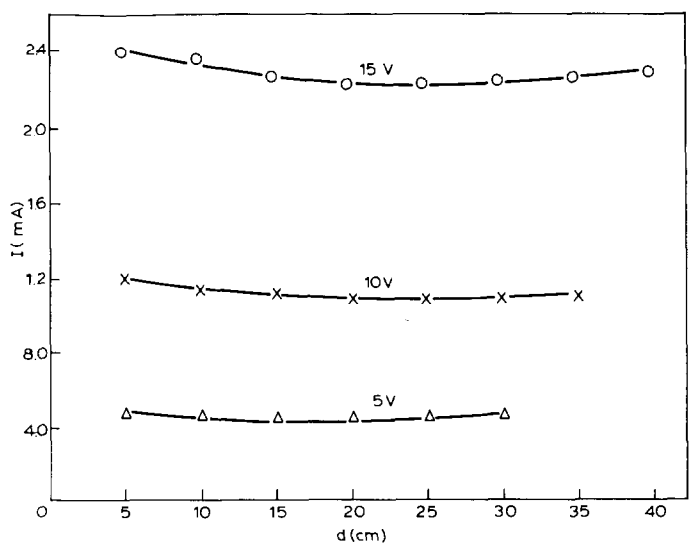

Fig. 5. Variation of the generated photoelectric current as a function of distance from the UV light source at various applied voltages.

Current–voltage characteristics at various temperatures

A point of interest is the non-linear dependence of current on voltage as shown in Fig. 6. This can be explained on the assumption that a blocking contact exists; at such contacts a space charge will be created in a depletion region due to the difference in the work functions of the metal and of the insulator. If there is an adequate density of donors, N_d (positive when empty), in this insulator, then electrons will be emitted from these states into the metal until thermomechanical equilibrium is achieved. This depletion region will extend to a distance λ and will give rise to an electric field in this region much higher than that in the bulk. The depletion region has a higher resistance than the rest of the bulk due to the absence of mobile carriers; the applied potential difference will almost entirely drop across this region. The electric field, E, and subsequently the field-lowering contact barrier $\Delta\phi$ are determined by the depletion width, λ, which, in turn, is determined by the density, N_d, of ionizable impurities according to the relation [10–12]

$$\lambda = \left(\frac{2\epsilon_0\epsilon_r V_c}{qN_d}\right)^{1/2} \approx 1.02\left(\frac{t_r V_c}{N_d}\right)^{1/2} \tag{1}$$

where V_c is the effective potential across the contact, $q = 1.6 \times 10^{-19}$ C, $\epsilon_0 = 8.854 \times 10^{-4}$ F cm^{-1} and ϵ_r is the relative dielectric constant. The

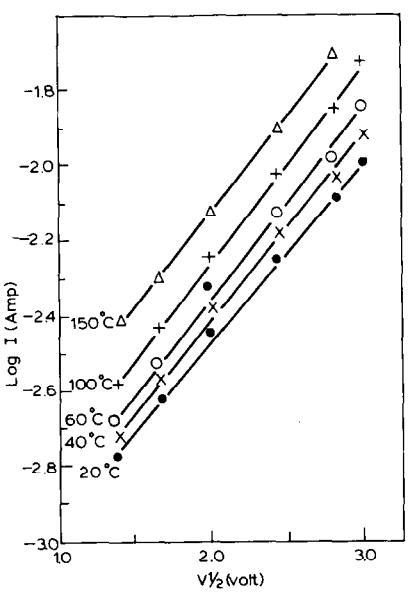

Fig. 6. Variation of the generated photoelectric current (log I) as a function of applied voltage ($V^{1/2}$) at various temperatures.

dielectric field at the contact is given by

$$E_c = \left(\frac{2qN_dV_c}{\epsilon_0\epsilon_r}\right)^{1/2} \approx 1.9 \times 10^{-3}\left(\frac{V_cN_d}{\epsilon_r}\right)^{1/2} \tag{2}$$

The current at low field varies with temperature in accordance with the equation

$$I = I_0 \exp^{-\Delta E/KT} \tag{3}$$

where ΔE is the activation energy for donors or traps, and

$$I_0 = q\mu N_d \frac{V}{d} A \tag{4}$$

where q is the electronic charge, μ is the mobility, N_d is the density of donors, V is the bias voltage, d is the effective electrode separation and A is the effective area. A plot of log I against $1000/T$ is shown in Fig. 7. The current at low field is proportional to temperature. According to eqns. (1) and (2) and Fig. 6, the average values of the parameters are N_d (donor concentration) $\approx 4.5 \times 10^{18}$ cm^{-3}, λ (depletion-layer thickness) $\approx 2.84 \times 10^{-6}$ cm.

Accordingly to eqn. (3) the gradient of these shapes yields a consistent value for the activation energy (Fig. 7, $\Delta E \approx 0.035$–0.078 eV), at different voltages.

From eqn. (4) and Fig. 7 the mobility of charge carriers was estimated to be 1.97×10^{-7} cm^2 V^{-1} s^{-1} and associated with a 0.078 eV activation energy at higher temperatures. This is an indication of a localized state conduction

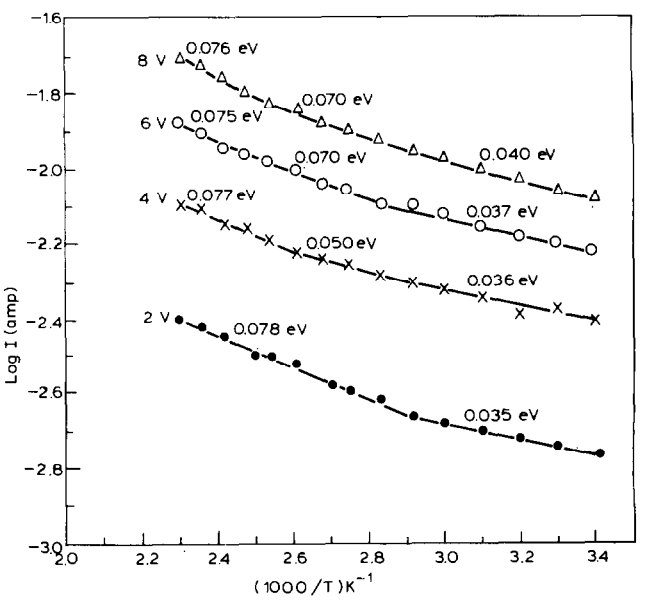

Fig. 7. Temperature ($1000/T$) dependence of the generated photoelectric current (log I) at various applied fields.

(hopping). The break of log I with $1/T$ is due to a change in activation energy to a higher value at higher temperatures.

Accordingly, amongst the new data evaluated in the present investigation, there is a conformity between the value of the activation energy calculated from the current–voltage relationship herein, and that previously determined from the temperature dependence of electrical resistivity [6].

REFERENCES

1 N.F. Mott, Philos. Mag., 19 (1969) 835; 22 (1970) 7; 24 (1971) 911.
2 M.H. Cohen, Proc. Semiconductor Effects in Amorphous Solids, North Holland, 1970.
3 P.W. Anderson, Phys. Rev., 109 (1958) 1492.
4 T.C. Harman, in D.G. Thomaś (Ed.), Proc. Int. Conf. Phys. II–VI Semiconductors, Brown University Providence, Benjamin, New York, 1967, p. 982.
5 R.A. Reynolds, C.G. Roberts, R.A. Chapman and H.B. Bebb, Proc. III. Int. Photoconductivity Conf., Stanford, 1969.
6 A. Tawfik, M.M. Abou Sekkina and M.I. Abd El-Ati, J. Mater. Sci., in press.
7 T. Furukawa and G.E. Johnson, J. Appl. Phys., 52 (1981) 940.
8 K., Weiser, R. Fisher and M.H. Brodsky, in S.P. Keller, J.C. Hessel and F. Stern (Eds.), Proc. 10th Conf. on the Physics of Semiconductors, Cambridge, Massachusetts, 1970, p. 667.
9 N.F. Mott and E.A. Davis, Electronic Process in Non-crystalline materials, Clarendon Press, Oxford, 1971.
10 G. Simmons, J. Phys. D, 4 (1971) 613.
11 A. Idem, Phys. Rev., 166 (1968) 912.
12 A. Idem, in L.I. Maissel and R. Glang (Eds.), Handbook of Thin Film Technology, McGraw-Hill, New York, 1970, Chap. 14.